



The Compact Muon Solenoid Experiment  
**Conference Report**

Mailing address: CMS CERN, CH-1211 GENEVA 23, Switzerland



27 January 2020 (v4, 09 August 2021)

# Azimuthal anisotropy and nuclear modification of Upsilon states in PbPb collisions with the CMS detector

Jaebeom Park for the CMS Collaboration

## Abstract

Bottomonia are produced by hard scattering in the early times of a relativistic heavy-ion collision, so they serve as excellent probes of the quark-gluon plasma (QGP). Early CMS data showed that the yields of the  $\Upsilon(1S)$ ,  $\Upsilon(2S)$ , and  $\Upsilon(3S)$  mesons are suppressed in PbPb relative to those in pp. In order to interpret the results in PbPb collision unambiguously, the cold nuclear matter effects need to be quantitatively estimated using pPb collisions data. Additionally, the measurement of the elliptic azimuthal anisotropy of bottomonium states have been suggested as a powerful tool to study the different in-medium effects such as dissociation and regeneration. In these proceedings, the new bottomonium results are reported for pPb and PbPb collisions data at 5.02 TeV with the CMS detector. First, the nuclear modification factors of the  $\Upsilon(1S)$ ,  $\Upsilon(2S)$ , and  $\Upsilon(3S)$  mesons are presented in pPb collisions as functions of the transverse momentum and rapidity. Then, the new measurements of the azimuthal anisotropy ( $v_2$ ) of the  $\Upsilon(1S)$  and  $\Upsilon(2S)$  mesons are reported using PbPb collisions data at 5.02 TeV taken in 2018.

Presented at *QuarkMatter2019 28th International Conference on Ultra-Relativistic Nucleus-Nucleus Collisions*,  
Published in *Nuclear Physics A 1005 (2021) 121875*, doi :10.1016/j.nuclphysa.2020.121875



XXVIIIth International Conference on Ultrarelativistic Nucleus-Nucleus Collisions  
(Quark Matter 2019)

## Azimuthal anisotropy and nuclear modification of Upsilon states in heavy-ion collisions with the CMS detector

JaeBeom Park (on behalf of the CMS Collaboration)<sup>a</sup>

<sup>a</sup>*Department of Physics, Korea University, Seoul, South Korea*

---

### Abstract

Bottomonia are produced by hard scattering in the early times of a relativistic heavy-ion collision, so they serve as excellent probes of the quark-gluon plasma (QGP). Early CMS data showed that the yields of the  $\Upsilon(1S)$ ,  $\Upsilon(2S)$ , and  $\Upsilon(3S)$  mesons are suppressed in PbPb relative to those in pp. In order to interpret the results in PbPb collision unambiguously, the cold nuclear matter effects need to be quantitatively estimated using pPb collisions data. Additionally, the measurement of the elliptic azimuthal anisotropy of bottomonium states have been suggested as a powerful tool to study the different in-medium effects such as dissociation and regeneration. In these proceedings, the new bottomonium results are reported for pPb and PbPb collisions data at 5.02 TeV with the CMS detector. First, the nuclear modification factors of the  $\Upsilon(1S)$ ,  $\Upsilon(2S)$ , and  $\Upsilon(3S)$  mesons are presented in pPb collisions as functions of the transverse momentum and rapidity. Then, the new measurements of the azimuthal anisotropy ( $v_2$ ) of the  $\Upsilon(1S)$  and  $\Upsilon(2S)$  mesons are reported using PbPb collisions data at 5.02 TeV taken in 2018.

*Keywords:*

---

### 1. Introduction

Quarkonia in relativistic heavy-ion collisions have been considered as golden probes for the study of strongly interacting matter of deconfined quarks and gluons, the quark-gluon plasma (QGP), at high energy-density and temperature [1]. Among various quarkonium states, bottomonia have short formation times in their rest frames [2] and are produced in the early stage of collisions via hard scattering. The yields are modified inside the QGP as a consequence of color-screening [3] and dissociation from inelastic parton scattering [4]. The LHC experiments CMS, ALICE, and ATLAS reported a significant suppression of the bottomonium states in lead-lead (PbPb) collisions at  $\sqrt{s_{NN}} = 5.02$  TeV [5, 6, 7]. In addition, the suppression of different bottomonium states has been observed in the ordering of their binding energy, which is consistent with the sequential melting picture of quarkonium suppression in the QGP [8]. In contrast to the Debye screening and dissociation, quarkonium yield can increase in the presence of QGP, by coalescence of uncorrelated quarks or recombination of heavy-quark pairs from an original dissociated quarkonium [9]. Since the number of heavy-quark pairs is much smaller for beauty than charm, compared to  $J/\psi$  studies the recombination processes is much smaller for  $\Upsilon$  mesons.

In addition to the in-medium QGP effects, the modification of the bottomonium production in PbPb collisions involves also the effects of the Pb nucleus itself, the so-called cold nuclear matter (CNM) effects. In order to separate the color screening effect alone, pPb collisions are performed in which the modification of the measured bottomonium yields is expected to be dominated by CNM effects. To estimate the CNM effects quantitatively, the nuclear modification factors  $R_{pPb}$  are measured defined as the ratios of bottomonium production cross sections in pPb collisions to that in pp collisions scaled by the number of nucleons in the Pb ion.

On the other hand, it has been suggested that the study of the azimuthal dependence of quarkonium states develops a more comprehensive understanding of the dynamics of quarkonia. The spatial anisotropy of the overlap region of the colliding nuclei in mid-central collisions is transformed into momentum anisotropy. This leads to a hydrodynamical anisotropic flow, which can be characterized as the second-order Fourier coefficients ( $v_2$ ) of the azimuthal particle distribution, known as the elliptic flow. A positive finite  $v_2$  has been observed for  $J/\psi$  mesons at LHC in both PbPb and pPb collisions [10, 11]. The  $v_2$  of the  $\Upsilon(1S)$  meson has been reported by ALICE Collaboration at forward rapidity in PbPb collisions.

In this conference proceedings, new results of  $R_{pPb}$  are described for  $\Upsilon(1S)$ ,  $\Upsilon(2S)$ , and  $\Upsilon(3S)$  mesons measured in pPb and pp collisions at 5.02 TeV. Also the  $v_2$  measurement of  $\Upsilon(1S)$  and  $\Upsilon(2S)$  mesons are reported in PbPb collisions at  $\sqrt{s_{NN}} = 5.02$  TeV.

## 2. Data and Event selection

The datasets used to obtain the  $R_{pPb}$  values are for pp and pPb collisions at  $\sqrt{s_{NN}} = 5.02$  TeV. The  $v_2$  of  $\Upsilon(1S)$  and  $\Upsilon(2S)$  mesons are measured using the data in PbPb collisions taken in late 2018. The detailed description of the CMS detector can be found in Ref. [12]. For both analyses, the  $\Upsilon$  mesons are reconstructed using the dimuon decay channel with single muons detected in the pseudorapidity interval of  $|\eta| < 2.4$ . The dimuon events are selected by a fast hardware-based trigger system, which requires two muon candidates based on the information from the muon detectors. No explicit momentum is required for the muons in pp and pPb collisions. The event selection trigger recorded an integrated luminosity of  $28 \text{ pb}^{-1}$  and  $34.6 \text{ nb}^{-1}$  in pp and pPb collisions, respectively. On the other hand, in the  $v_2$  analysis, the two muon candidates require track fits in the outer muon spectrometer with applying a transverse momentum cut on one of the muon to be larger than  $2 \text{ GeV}/c$ . In addition, the other muon is reconstructed using full tracks from tracks in the outer muon spectrometer and the inner tracker information, with a minimum of 10 high-quality hits in the inner tracker and a minimum  $p_T$  threshold at  $2 \text{ GeV}/c$ . Finally, the events are selected with the invariant mass of the two muons being larger than  $7 \text{ GeV}/c^2$ . The recorded integrated luminosity of the trigger used for the  $v_2$  analysis is  $1.7 \text{ nb}^{-1}$ . Muons used in pp and pPb collisions are selected in the kinematic range of  $p_T > 4 \text{ GeV}/c$  and  $|\eta| < 2.4$ , and the dimuons are studied in  $p_T < 30 \text{ GeV}/c$  and  $|\eta^{\mu\mu}| < 2.4$ . In PbPb collisions, the single muon  $p_T$  cut is loosened to  $3.5 \text{ GeV}/c$  and the dimuon  $p_T$  range is increased up to  $50 \text{ GeV}$ , while the  $\eta$  and  $y$  selection is kept the same.

## 3. Analysis procedure

The yields of the  $\Upsilon$  states in pp and pPb collisions are extracted using an unbinned maximum-likelihood fit to the invariant mass spectra within  $8\text{--}14 \text{ GeV}/c^2$  with a signal PDF and background PDF. The sum of two Crystal Ball (CB) functions is used for the signal PDF and an error function multiplied by an exponential function for the background PDF. The elliptic flow signal  $v_2$  values of the  $\Upsilon$  candidates in PbPb collisions are obtained using the scalar product (SP) method [13]. The event plane angles in this method are characterized by  $Q$ -vectors that are determined in different pseudorapidity ranges using the tracks in mid-rapidity region or the HF calorimeters located in  $3 < |\eta| < 5$ . In order to separate the signal and background in the  $v_2$  distribution, the invariant mass and  $v_2$  spectrum of  $\Upsilon$  candidates are fitted simultaneously. The same signal and background functions are used to describe the mass distribution as in pp and pPb collisions. The dependence of the  $v_2$  profile on the dimuon mass ( $m_{inv}$ ) is taken as

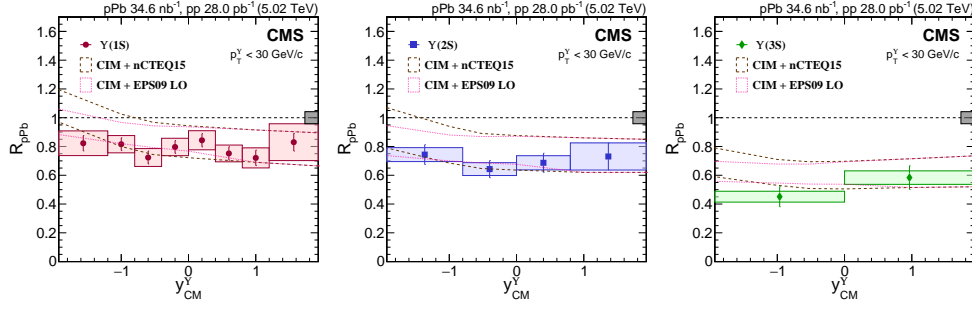


Fig. 1.  $R_{pPb}$  versus  $y_{CM}$  [17] with comover effect predictions from E. Ferreiro and J. Lansberg [14] with shadowing corrections using nCTEQ15 and EPS09 for  $\Upsilon(1S)$  (left),  $\Upsilon(2S)$  (middle) and  $\Upsilon(3S)$  (right). The final-state comover effect is seen to modify the  $\Upsilon$  states sequentially. Error bars on the points represent statistical and fit uncertainties and filled boxes represent systematic uncertainties. The gray box around the line at unity represents the global uncertainty due to luminosity normalization.

$$v_2(m_{inv}) = \alpha_1(m_{inv})v_2^{\Upsilon(1S)} + \alpha_2(m_{inv})v_2^{\Upsilon(2S)} + \alpha_3(m_{inv})v_2^{\Upsilon(3S)} + [1 - \alpha_1(m_{inv}) - \alpha_2(m_{inv}) - \alpha_3(m_{inv})]v_2^{Bkg}(m_{inv}), \quad (1)$$

where

$$\alpha_n(m_{inv}) = [Sig_{\Upsilon(nS)}] / [Sig_{\Upsilon(1S)}(m_{inv}) + Sig_{\Upsilon(2S)}(m_{inv}) + Sig_{\Upsilon(3S)}(m_{inv}) + Bkg(m_{inv})] \quad (n = 1, 2, 3). \quad (2)$$

#### 4. Results

The values of  $R_{pPb}$  in pPb collisions for  $\Upsilon(1S)$ ,  $\Upsilon(2S)$ , and  $\Upsilon(3S)$  mesons are calculated using the ratio of measured yields in pPb collisions to that in pp collisions scaled by the number of nucleons in the Pb ion. The normalized yields in pp and pPb collisions are obtained using the fit to the dimuon mass spectrum detailed in Sec. 3. Figure 1 shows the  $R_{pPb}$  values as a function of dimuon rapidity in the center-of-mass frame ( $y_{CM}$ ).  $\Upsilon(1S)$ ,  $\Upsilon(2S)$ , and  $\Upsilon(3S)$  mesons are observed to be suppressed in pPb collisions compared to pp collisions in all studied rapidity ranges. Also, the amount of suppression is in the order of the binding energy of the  $\Upsilon$  states. Also, the results are compared with the predictions using the comover interaction model (CIM) [14] with two different leading-order nPDF calculations from EPS09 [15] and nCTEQ15 [16]. The CIM suggests stronger modification for the excited states due to their larger size which increases the cross section for comover interaction. The  $v_2$  results of  $\Upsilon(1S)$  and  $\Upsilon(2S)$  mesons are shown in Fig. 2. The left panel shows the results in four centrality intervals for  $\Upsilon(1S)$  mesons and the values are found to be consistent with zero. The rightmost points are the average  $v_2$  values in the 10–90% centrality interval for  $\Upsilon(1S)$  and  $\Upsilon(2S)$  mesons. Both values are consistent with zero and the  $v_2$  value for  $\Upsilon(1S)$  meson in that bin is determined to be  $0.007 \pm 0.011$  (stat)  $\pm 0.005$  (syst). The right panel of Fig. 2 shows the  $v_2$  of  $\Upsilon(1S)$  mesons as a function of  $p_T$  in the centrality interval 10–90% the results are consistent with zero in all studied  $p_T$  bins. The 0–10% interval is excluded in this plot due to the small eccentricity by the circular shape of the collision geometry in the transverse plane. The plot is also compared to four different theory calculations with different ingredients such as in-medium effects like regeneration and initial temperature of the QGP.

#### 5. Summary

The nuclear modification factors  $R_{pPb}$  are measured for  $\Upsilon(1S)$ ,  $\Upsilon(2S)$ , and  $\Upsilon(3S)$  mesons. All three states are found to be suppressed in pPb collisions, sequentially in the ordering of their binding energy, which can be explained by final state effects such as dissociation from comover interactions. The modification of bottomonium states in pPb collisions is much smaller than that in PbPb collisions, indicating the suppression in PbPb collisions is dominated by the in-medium effects of the QGP. The  $v_2$  of  $\Upsilon(1S)$  mesons is measured as

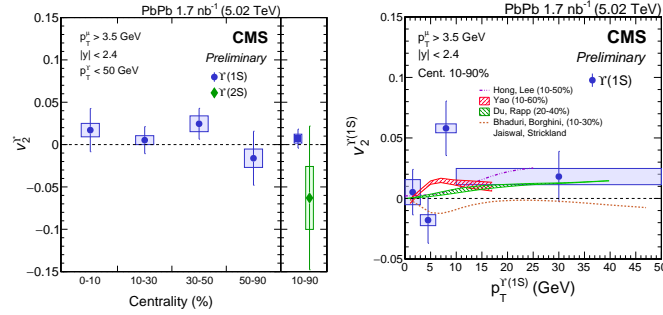


Fig. 2. (Left)  $p_T$  integrated  $v_2$  values for  $\Upsilon(1S)$  mesons measured in four centrality bins and for the  $\Upsilon(2S)$  meson in the 10-90% centrality range [18]. (Right)  $v_2$  as a function of  $p_T$  in the 10-90% centrality range compared with model calculations from Du and Rapp (Green shaded area) [9], from Hong and Lee (dashed violet line) [19], from Yao (red band) [20], and from Bhadury, Borghini, Jaiswal and Strickland (dashed brown line) [21]. All results are for the rapidity range of  $|y| < 2.4$ . The vertical bars denote statistical uncertainties, and the rectangular bands show the total systematic uncertainties.

a function of  $p_T$  and PbPb collision centrality. The  $v_2$  values have been measured with the highest precision achieved to date. The observation that the  $v_2$  of the  $\Upsilon$  states are small and consistent with zero contrasts with the previously measured  $J/\psi$   $v_2$  results, suggesting different medium effects for charmonia and bottomonia. Recent calculations predict a larger  $v_2$  value for  $\Upsilon(2S)$  mesons compared to  $\Upsilon(1S)$ , resulting from differences in the degree to which regeneration processes contribute to their respective production.

## References

- [1] F. Karsch, E. Laermann, Thermodynamics and in-medium hadron properties from lattice QCD, in: R. C. Hwa, X.-N. Wang (Eds.), Quark-Gluon Plasma III, World Scientific Publishing Co. Pte. Ltd., 2004. arXiv:hep-lat/0305025.
- [2] K. Geiger, Qcd space-time analysis of quarkonium formation and evolution in hadronic collisions, Phys. Rev. D 57 (1998) 1895. doi:10.1103/PhysRevD.57.1895.
- [3] T. Matsui, H. Satz,  $J/\psi$  suppression by quark-gluon plasma formation, Phys. Lett. B 178 (1986) 416.
- [4] N. Brambilla, et al., Static quark-antiquark pairs at finite temperature, Phys. Rev. D 78 (2008) 014017.
- [5] CMS Collaboration, Measurement of nuclear modification factors of  $\Upsilon(1S)$ ,  $\Upsilon(1S)$ , and  $\Upsilon(1S)$  mesons in PbPb collisions at  $\sqrt{s_{NN}} = 5.02$  TeV, Phys. Lett. B 790 270.
- [6] ALICE Collaboration,  $\Upsilon$  suppression at forward rapidity in PbPb collisions at  $\sqrt{s_{NN}} = 5.02$  TeV, Phys. Lett. B 790 89.
- [7] Production of  $\Upsilon(nS)$  mesons in Pb+Pb and  $pp$  collisions at 5.02 TeV with ATLAS, Tech. Rep. ATLAS-CONF-2019-054, CERN.
- [8] M. Strickland, D. Bazow, Thermal bottomonium suppression at RHIC and LHC, Nuclear Physics A 879 (2012) 25.
- [9] X. Du, et al., Color screening and regeneration of bottomonia in high-energy heavy-ion collisions, Phys. Rev. C 96 (2017) 054901.
- [10] ALICE Collaboration,  $J/\psi$  Elliptic Flow in Pb-Pb Collisions at  $\sqrt{s_{NN}} = 5.02$  TeV, Phys. Rev. Lett. 119 (2017) 242301.
- [11] CMS Collaboration, Observation of prompt  $J/\psi$  meson elliptic flow in high-multiplicity pPb collisions at  $\sqrt{s_{NN}} = 8.16$  TeV, Phys. Lett. B 791 (2019) 172.
- [12] CMS Collaboration, The CMS experiment at the CERN LHC, Journal of Instrumentation 3 (08) (2008) S08004.
- [13] STAR Collaboration, Elliptic flow from two- and four-particle correlations in Au+Au collisions at  $\sqrt{s_{NN}} = 130$  GeV, Phys. Rev. C 66 (2002) 034904.
- [14] E. G. Ferreira, J. P. Lansberg, Is bottomonium suppression in proton-nucleus and nucleus-nucleus collisions at LHC energies due to the same effects?, Journal of High Energy Physics 2018 (10) (2018) 94.
- [15] K. Eskola, H. Paukkunen, C. Salgado, EPS09 — A new generation of NLO and LO nuclear parton distribution functions, Journal of High Energy Physics 2009 (04) (2009) 065.
- [16] K. Kovarik, et al., nCTEQ15: Global analysis of nuclear parton distributions with uncertainties in the CTEQ framework, Phys. Rev. D 93 (2016) 085037.
- [17] Nuclear modification of  $\Upsilon$  states in pPb collisions at  $\sqrt{s_{NN}} = 5.02$  TeV, Tech. Rep. CMS-PAS-HIN-18-005, CERN. URL <http://cds.cern.ch/record/2699566>
- [18] Measurement of the elliptic flow of  $\Upsilon(1S)$  and  $\Upsilon(2S)$  mesons in PbPb collisions at  $\sqrt{s_{NN}} = 5.02$  TeV, Tech. Rep. CMS-PAS-HIN-19-002, CERN. URL <http://cds.cern.ch/record/2698580>
- [19] J. Hong, S. H. Lee,  $\Upsilon(1S)$  transverse momentum spectra through dissociation and regeneration in heavy-ion collisions, Phys. Lett. B 801 (2020) 135147.
- [20] X. Yao, et al., Quarkonium production in heavy ion collisions: coupled Boltzmann transport equations, Nuclear Physics A 982 (2019) 755, the 27th International Conference on Ultrarelativistic Nucleus-Nucleus Collisions: Quark Matter 2018.
- [21] P. P. Bhaduri, N. Borghini, A. Jaiswal, M. Strickland, Anisotropic escape mechanism and elliptic flow of bottomonium arXiv:1809.06235.